Strong correlation and anticorrelation via quantum coherence in a cascade atom with split metastable states

Xiang-ming Hu and Fei Wang
Department of Physics, Huazhong Normal University, Wuhan 430079, People's Republic of China
(Received 3 February 2007; published 26 June 2007)

We show that strongly correlated and anticorrelated photons can be produced from two fluorescent fields emitted by a driven cascade atom with split metastable states. Depending on the choice of parameters, we have strong correlations for both fluorescent fields, anticorrelations for both, and strong correlation for one and anticorrelation for the other. In the presence of level splitting, we have two interfering cascade-dressed transitions from the top state to the antisymmetric superposition of the metastable states. The interference between the two cascade-dressed transitions is responsible for the strong correlations and anticorrelations.

DOI: 10.1103/PhysRevA.75.065802 PACS number(s): 42.50.Ct, 32.80.Qk, 42.50.Lc

Quantum coherence and interference have led to many effects such as coherent population trapping (CPT) [1], electromagnetic-induced transparency [2–5], lasing without inversion [6–9], and modification of spontaneous emission [10–14]. Recently, much attention has been paid to the effects of quantum coherence on the coherent manipulation of photon correlations. The photon correlation is described by the normalized two-time intensity correlation function. It is well known that for a chaotic light, the intensity correlation function decays monotonously from 2 to 1 as time separation increases [15]. For fluorescent photons from strongly driven two-level atoms [16], the intensity correlation function rises from zero to its maximal value smaller than 2 and drops to a value between zero and unity, and then rises. After several oscillations, the correlation function tends to unity. When quantum coherence and interference are utilized, the photon correlations are remarkably modified. The intensity correlation function takes extremely large values (much larger than 2) or remains below unity for a long time (many periods of oscillations or all times) [17–20]. For the convenience of discrimination, in the present paper we refer to the former as *strong correlation* while to the latter as *anticorrelation*. Swain *et al.* [17] showed that both strong correlation and anticorrelation occur for the same fluorescent field but for different parameters in a three-level V atom, in which the quantum interference arises from the coupling of the two near-degenerate transitions to the same vacuum modes. This requires that these two transition dipoles have the parallel components—that is, the two excited states have the same quantum numbers J and m_J. This condition is stringent and is difficult to find in realistic systems. Later, Ficek and Swain [18] proposed to use a dc field to couple the decaying state to an auxiliary state and to realize the interference in the dressed-state representation. For the equivalent realization of quantum interference, a strict limitation was still imposed on the equivalent systems; that is, the auxiliary state must be metastable. If the auxiliary state is not metastable—for example, it decays at a rate that is comparable to that for the excited state under consideration—the correlation function falls back to the normal level. It is the very case for a resonantly driven three-level atom in the cascade configuration [21]. In order to overcome this difficulty, we proposed to tune the driving fields far off resonance with the corresponding one-photon transitions [19]. In this case, the ground state serves as a metastable state. It is also for this reason that a three-level Λ atom (with near-degenerate metastable states but without parallel dipole moments) is a good candidate for the strong correlation when it operates near but not exactly at CPT [20]. Physically, both strong correlation and anticorrelation have the same origin, the atomic coherence, which is created due to the CPT effect. If an atom is trapped almost but not totally in the ground states and it decays rapidly, this gives rise to the strong correlation. However, when an atom tends to be trapped in the excited states and it decays at a small rate, this results in anticorrelation.

Here we extend the study of the intensity correlations for the driven cascade atom [21] by taking lower-level splitting into account. It is shown that lower-level splitting can be used to manipulate the photon correlations for cascade transitions. The atom is driven by three fields, of which one is resonantly coupled to the upper transition and the other two are tuned to the average frequency of the two lower transitions in the Λ configuration. When the Λ subsystem operates near CPT, the atomic coherence, which is created between the two ground states, has its effects on the correlations for the fluorescent fields from the cascade transitions. The strongly correlated or anticorrelated photons are produced from the two fluorescent fields emitted from the cascade transitions. For an appropriate choice of parameters, we have strong correlations for both fluorescent fields, anticorrelations for both, or strong correlation for one and anticorrelation for the other. Both the strong correlation and the anticorrelation can be obtained when the driving fields are strong. This is in sharp contrast to the case without lower-level splitting [21], in which the correlations for both the upper and lower transitions are at a normal level.

The present system is shown in Fig. 1(a). For simplicity we consider only two closely spaced, metastable states $|1\rangle$ and $|2\rangle$, which are generated due to couplings such as Zeeman splitting. The transitions $|1,2\rangle$-$|3\rangle$ and $|3\rangle$-$|4\rangle$ are electronic dipole allowed, while the transitions $|1\rangle$-$|2,4\rangle$ and $|2\rangle$-$|4\rangle$ are electronic dipole forbidden. The atom is driven on the lower transitions $|1,2\rangle$-$|3\rangle$ in the Λ configuration by two lasers of the same frequency ω_1 and on the upper transition $|3\rangle$-$|4\rangle$ by one laser of frequency ω_2. The master equation for the reduced density operator ρ is derived in an appropriate rotating frame and in the dipole approximation as [22]

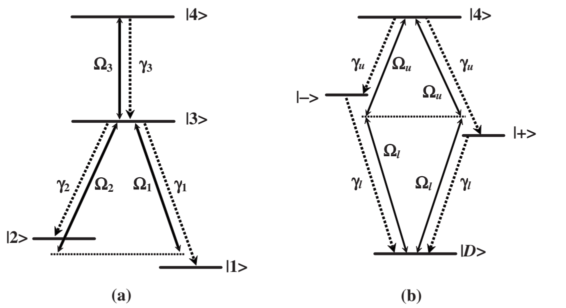

FIG. 1. (a) Four-level atomic system. Ω_k $(k=1,2,3)$ are the Rabi frequencies for the atom-field interactions, and γ_k are the atomic decay rates. (b) The interfering channels in the dressed-state representation as described in the text. $\Omega_{u,l}$ are the Rabi frequencies for the upper and lower transitions, respectively, and $\gamma_{u,l}$ are the atomic decay rates for the upper and lower transitions, respectively.

$$\dot{\rho} = -\frac{i}{\hbar}[H_1 + H_2, \rho] + \mathcal{L}_{13}\rho + \mathcal{L}_{23}\rho + \mathcal{L}_{34}\rho, \tag{1}$$

where H_1 and H_2 describe the interactions on the transitions $|1,2\rangle$-$|3\rangle$ and $|3\rangle$-$|4\rangle$,

$$H_1 = -\hbar\Delta_1\hbar\sigma_{11} + \hbar(\omega_{21} - \Delta_1) - \frac{\hbar}{2}(\Omega_1\sigma_{13} + \Omega_2\sigma_{23} + \text{H.c.}), \tag{2}$$

$$H_2 = \hbar\Delta_2\sigma_{44} - \frac{\hbar}{2}\Omega_3(\sigma_{34} + \sigma_{43}), \tag{3}$$

and the damping terms take the form

$$\mathcal{L}_{ij}\rho = \frac{\gamma_i}{2}(2\sigma_{ij}\rho\sigma_{ji} - \sigma_{jj}\rho - \rho\sigma_{jj}). \tag{4}$$

In Eqs. (1)–(4), $\sigma_{ij}=|i\rangle\langle j|$ represent the atomic projection operators for $i=j$ and the flip operators for $i\neq j$ $(i,j=1-4)$. By $\Delta_1=\omega_{31}-\omega_1$ and $\Delta_2=\omega_{43}-\omega_2$ we denote the atom-field detunings, where ω_{ij} are the atomic resonance frequencies. Ω_k $(k=1,2,3)$ are the Rabi frequencies for the atom-field interactions, and γ_k are the atomic decay rates. Without loss of generality, we assume that the Rabi frequencies are real because of the absence of a closed loop of the coherent transitions. The set of equations for the density matrix elements are derived from Eqs. (1)–(4) as

$$\dot{\rho}_{11} = \gamma_1\rho_{33} + \frac{i}{2}\Omega_1(\rho_{31} - \rho_{13}), \tag{5}$$

$$\dot{\rho}_{22} = \gamma_2\rho_{33} + \frac{i}{2}\Omega_2(\rho_{32} - \rho_{23}), \tag{6}$$

$$\dot{\rho}_{44} = -\gamma_3\rho_{44} + \frac{i}{2}\Omega_3(\rho_{34} - \rho_{43}), \tag{7}$$

$$\dot{\rho}_{12} = i\omega_{21}\rho_{12} - \frac{i}{2}\Omega_2\rho_{13} + \frac{i}{2}\Omega_1\rho_{32}, \tag{8}$$

$$\dot{\rho}_{13} = -\left[\frac{1}{2}(\gamma_1 + \gamma_2) - i\Delta_1\right]\rho_{13} - \frac{i}{2}\Omega_2\rho_{12} - \frac{i}{2}\Omega_1(\rho_{11} - \rho_{33}) - \frac{i}{2}\Omega_3\rho_{14}, \tag{9}$$

$$\dot{\rho}_{14} = -\left[\frac{1}{2}\gamma_3 - i(\Delta_2 + \Delta_1)\right]\rho_{14} - \frac{i}{2}\Omega_3\rho_{13} + \frac{i}{2}\Omega_1\rho_{34}, \tag{10}$$

$$\dot{\rho}_{23} = -\left[\frac{1}{2}(\gamma_1 + \gamma_2) - i(\Delta_1 - \omega_{21})\right]\rho_{23} - \frac{i}{2}\Omega_1\rho_{21} - \frac{i}{2}\Omega_2(\rho_{22} - \rho_{33}) - \frac{i}{2}\Omega_3\rho_{24}, \tag{11}$$

$$\dot{\rho}_{24} = -\left[\frac{1}{2}\gamma_3 - i\Delta_2 - i(\Delta_1 - \omega_{21})\right]\rho_{24} - \frac{i}{2}\Omega_3\rho_{23} + \frac{i}{2}\Omega_2\rho_{34}, \tag{12}$$

$$\dot{\rho}_{34} = -\left[\frac{1}{2}(\gamma_1 + \gamma_2 + \gamma_3) - i\Delta_2\right]\rho_{34} - \frac{i}{2}\Omega_3(\rho_{33} - \rho_{44}) + \frac{i}{2}\Omega_1\rho_{14} + \frac{i}{2}\Omega_2\rho_{24}, \tag{13}$$

together with the complex conjugates of Eqs. (8)–(13). The closure of the system requires that $\rho_{11}+\rho_{22}+\rho_{33}+\rho_{44}=1$.

The normalized intensity correlation functions of the fluorescent fields are given by [15]

$$g_{ij}^{(2)}(\tau) = \lim_{t\to\infty}\frac{\langle E_i^{(-)}(t)E_j^{(-)}(t+\tau)E_j^{(+)}(t+\tau)E_i^{(+)}(t)\rangle}{\langle E_i^{(-)}(t)E_i^{(+)}(t)\rangle\langle E_j^{(-)}(t)E_j^{(+)}(t)\rangle}, \tag{14}$$

where $i,j=1,2$. Here $E_i^{(-)}(t)$ and $E_i^{(+)}(t)$ are the negative and positive frequency parts of the fluorescent field operators, respectively. Relating the fluorescent field operators to the atomic flip operators, we have $E_1^{(+)}(t) \propto D_1(t)=\vec{\mu}_1\sigma_{13}(t)+\vec{\mu}_2\sigma_{23}(t)$, $E_2^{(+)}(t)\propto D_2(t)=\vec{\mu}_3\sigma_{34}(t)$ and $E_1^{(-)}(t)\propto D_1^{\dagger}(t)$, $E_2^{(-)}(t)\propto D_2^{\dagger}(t)$, where $\vec{\mu}_i$ $(i=1,2,3)$ are the electronic dipole moments for the transitions $|1,2\rangle$-$|3\rangle$ and $|3\rangle$-$|4\rangle$, respectively. The correlation function for the lower transitions takes the form

$$g_{11}^{(2)}(\tau) = \lim_{t\to\infty}\frac{\langle D_1^{\dagger}(t)\sigma_{33}(t+\tau)D_1(t)\rangle}{(|\vec{\mu}_1|^2 + |\vec{\mu}_2|^2)\langle\sigma_{33}(t)\rangle\langle\sigma_{33}(t+\tau)\rangle}. \tag{15}$$

By quantum regression theory [23], the correlation functions $\langle D_1^{\dagger}(t)\sigma_{ij}(t+\tau)D_1(t)\rangle$ follow exactly the same set of equations with respect to time τ for the density matrix elements $\rho_{ji}(\tau)$ with initial conditions $\rho_{ji}(0)\langle\sigma_{33}(t)\rangle$, where we have $\rho_{ji}(0)=0$ except for

$$\rho_{11}(0) = \frac{\gamma_1}{\gamma_1 + \gamma_2}, \quad \rho_{22}(0) = \frac{\gamma_2}{\gamma_1 + \gamma_2}. \tag{16}$$

With the above initial conditions, the correlation function for the fluorescent field $E_1(t)$ is written as

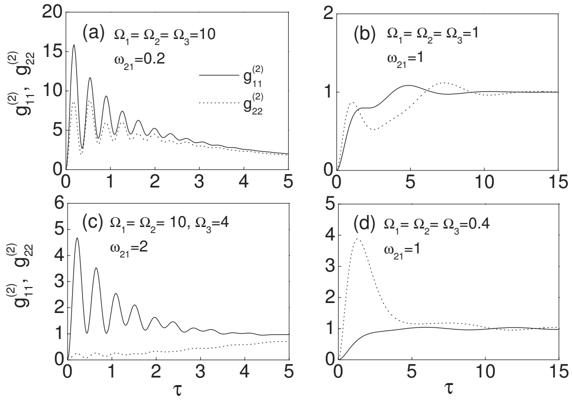

FIG. 2. Intensity correlation functions $g_{11}^{(2)}(\tau)$ (solid lines) and $g_{22}^{(2)}(\tau)$ (dotted lines) for (a) $\Omega_1=\Omega_2=\Omega_3=10$, $\omega_{21}=0.2$; (b) $\Omega_1=\Omega_2=\Omega_3=1$, $\omega_{21}=1$; (c) $\Omega_1=\Omega_2=10$, $\Omega_3=4$, $\omega_{21}=2$; and (d) $\Omega_1=\Omega_2=\Omega_3=0.4$, $\omega_{21}=1$.

$$g_{11}^{(2)}(\tau)=\left.\frac{\rho_{33}(\tau)}{\rho_{33}(\infty)}\right|_{\rho_{ji}(0)}, \tag{17}$$

where $\rho_{33}(\tau)$ and $\rho_{33}(\infty)$ are the transient and steady-state populations at level $|3\rangle$, respectively. In the same way, by using the transient and steady-state populations $\rho_{44}(\tau)$ and $\rho_{44}(\infty)$ at level $|4\rangle$, we obtain the correlation function for the fluorescent field $E_2(t)$ as

$$g_{22}^{(2)}(\tau)=\left.\frac{\rho_{44}(\tau)}{\rho_{44}(\infty)}\right|_{\rho_{ji}(0)}, \tag{18}$$

with the initial conditions $\rho_{ji}(0)=0$ except for $\rho_{33}(0)=1$.

In what follows we present the numerical results. The Rabi frequencies, the detunings, and the decay rates are scaled in units of γ_1 and the time is in units of γ_1^{-1}. We choose the parameters as $\gamma_2=\gamma_3=1$, $\Delta_1=\frac{1}{2}\omega_{21}$, and $\Delta_2=0$. In Fig. 2 we plot the correlation functions $g_{11}^{(2)}(\tau)$ (solid lines) and $g_{22}^{(2)}(\tau)$ (dashed lines) for (a) $\Omega_1=\Omega_2=\Omega_3=10$, $\omega_{21}=0.2$, (b) $\Omega_1=\Omega_2=\Omega_3=1$, $\omega_{21}=1$, (c) $\Omega_1=\Omega_2=10$, $\Omega_3=4$, $\omega_{21}=2$, and (d) $\Omega_1=\Omega_2=\Omega_3=0.4$, $\omega_{21}=1$. The remarkable features are presented as follows.

(1) *Strong correlations for both fluorescent fields*. In Fig. 2(a), the correlation functions take their maximal values $[g_{11}^{(2)}]_{\max}=15.88$ and $[g_{22}^{(2)}]_{\max}=8.69$ at $\tau=0.18$. The numerical calculations show that both fluorescent fields have strong correlations when $\omega_{21}\ll\gamma_1\ll(\Omega_1,\Omega_2)$.

(2) *Anticorrelations for both fluorescent fields*. In Fig. 2(b), $g_{11}^{(2)}(\tau)$ and $g_{22}^{(2)}(\tau)$ remain below unity for $\tau\approx3.8$ and $\tau\approx6.0$, respectively. In general, this appears when $\omega_{21}\sim\gamma_1\sim(\Omega_1,\Omega_2,\Omega_3)$.

(3) *Strong correlation for one fluorescent field and anticorrelation for the other*. In Fig. 2(c), $g_{11}^{(2)}(\tau)$ has its maximal value $[g_{11}^{(2)}]_{\max}=4.68$ at $\tau=0.22$, while $g_{22}^{(2)}(\tau)$ remains below unity for all times. This is achieved when $(\gamma_j\lesssim\omega_{21})\ll\Omega_3\ll(\Omega_1,\Omega_2)$. In Fig. 2(d), $g_{11}^{(2)}(\tau)$ remains below unity for $\tau\approx4.6$, while $g_{22}^{(2)}(\tau)$ has its maximal value $[g_{22}^{(2)}]_{\max}=3.88$ at $\tau=1.32$. The corresponding conditions are $(\Omega_1,\Omega_2,\Omega_3)\ll\omega_{21}\lesssim\gamma_1$. It should be noted that the anticorrelation and the strong correlation appear when the driving fields are strong and weak, respectively. This is in sharp contrast to the usual case of the two-level system, where anticorrelation only appears for a weak driving field and the correlation at the normal level is for the strong driving field.

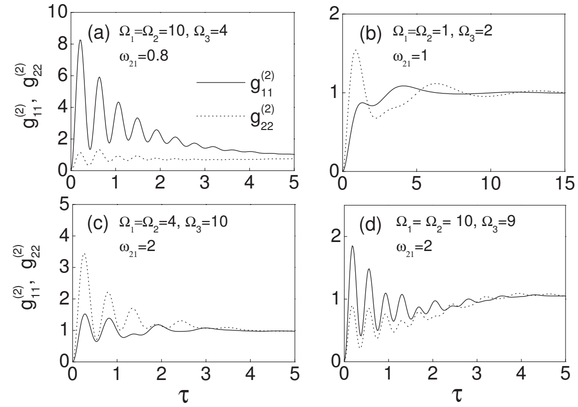

FIG. 3. Intensity correlation functions $g_{11}^{(2)}(\tau)$ (solid lines) and $g_{22}^{(2)}(\tau)$ (dot lines) for (a) $\Omega_1=\Omega_2=10$, $\Omega_3=4$, $\omega_{21}=0.8$; (b) $\Omega_1=\Omega_2=1$, $\Omega_3=2$, $\omega_{21}=1$; (c) $\Omega_1=\Omega_2=4$, $\Omega_3=10$, $\omega_{21}=2$; and (d) $\Omega_1=\Omega_2=10$, $\Omega_3=9$, $\omega_{21}=2$.

When the above conditions are relaxed, we have the strong correlation or the anticorrelation for one fluorescent field and the normal correlation for the other. In Fig. 3 we plot the correlation functions $g_{11}^{(2)}(\tau)$ (solid lines) and $g_{22}^{(2)}(\tau)$ (dashed lines) for (a) $\Omega_1=\Omega_2=10$, $\Omega_3=4$, $\omega_{21}=0.8$; (b) $\Omega_1=\Omega_2=1$, $\Omega_3=2$, $\omega_{21}=1$; (c) $\Omega_1=\Omega_2=4$, $\Omega_3=10$, $\omega_{21}=2$; and (d) $\Omega_1=\Omega_2=10$, $\Omega_3=9$, $\omega_{21}=2$. From this figure we have (a) $[g_{11}^{(2)}]_{\max}=8.25$ at $\tau=0.2$, (b) $g_{11}^{(2)}<1$ for $\tau=3.1$, (c) $[g_{22}^{(2)}]_{\max}=3.46$ at $\tau=0.26$, and (d) $g_{22}^{(2)}<1$ for $\tau=3.06$.

The above phenomena can be understood in terms of dressed states. The present system operates near but not exactly at CPT. The perturbation is caused by the level spacing ω_{21}, as shown in what follows. For simplicity we assume $\Omega_1=\Omega_2=\Omega$, $\Delta_1=\frac{1}{2}\omega_{21}$, and $\gamma_1=\gamma_2=\gamma_3$. We introduce the symmetric and antisymmetric states $|B\rangle=\frac{1}{\sqrt{2}}(|1\rangle+|2\rangle)$ and $|D\rangle=\frac{1}{\sqrt{2}}(|1\rangle-|2\rangle)$, in terms of which the Hamiltonian H_1 is rewritten as

$$H_1=-\frac{\hbar}{2}\omega_{21}(\sigma_{BD}+\sigma_{DB})-\frac{\hbar}{2}\sqrt{2}\Omega(\sigma_{3B}+\sigma_{B3}), \tag{19}$$

where the former term describes the coupling between the symmetric and antisymmetric states $|B\rangle$ and $|D\rangle$ with the effective Rabi frequency ω_{21}, and the latter term presents the coupling between the symmetric state $|B\rangle$ and the middle state $|3\rangle$ with Rabi frequency $\sqrt{2}\Omega$. Once $\omega_{21}=0$, the antisymmetric state $|D\rangle$ is decoupled from the system and acts as a dark state, where the atom is trapped. Here we focus on the case of $\omega_{21}\neq0$. By diagonalizing the second term of the Hamiltonian H_1, we have the dressed states $|\pm\rangle=\frac{1}{\sqrt{2}}(\pm|B\rangle+|3\rangle)$. In the new basis $(|D\rangle,|\pm\rangle,|4\rangle)$ we rewrite the Hamiltonians H_1 and H_2 as

$$H_1 = \frac{\hbar}{2}\omega_{-+}(\sigma_{--} - \sigma_{++}) - \frac{\hbar}{2}\Omega_l(\sigma_{+D} + \sigma_{-D} + \text{H.c.}), \quad (20)$$

$$H_2 = -\frac{\hbar}{2}\Omega_u(\sigma_{+4} + \sigma_{-4} + \text{H.c.}). \quad (21)$$

In Eq. (20), the first term describes the dressed states $|\pm\rangle$ with level spacing $\omega_{-+}=\sqrt{2}\Omega$ and the second term describes the coherent couplings between the states $|\pm\rangle$ and $|D\rangle$ with Rabi frequency $\Omega_l=\frac{\omega_{21}}{\sqrt{2}}$. Equation (21) denotes the couplings between the states $|\pm\rangle$ and $|4\rangle$ with Rabi frequency $\Omega_u=\frac{\Omega_3}{\sqrt{2}}$. The dressed transitions are plotted in Fig. 1(b).

Similarly, in the new basis $(|D\rangle,|\pm\rangle,|4\rangle)$ we obtain the cross damping terms from the damping terms in Eq. (1) as

$$\mathcal{L}^{(l)}_{+-}\rho = \frac{\gamma_l}{2}(2\sigma_{D+}\rho\sigma_{-D} - \sigma_{-+}\rho - \rho\sigma_{-+}) + (- \leftrightarrow +), \quad (22)$$

$$\mathcal{L}^{(u)}_{+-}\rho = \gamma_u(\sigma_{+4}\rho\sigma_{4-} + \sigma_{-4}\rho\sigma_{4+}), \quad (23)$$

where $\gamma_{u,l}=\frac{\gamma_1}{2}$. Equations (22) and (23) show that quantum interference appears between the dressed transitions $|\pm\rangle \rightsquigarrow |D\rangle$ in the V configuration [24] and between the dressed transitions $|4\rangle \rightsquigarrow |\pm\rangle$ in the Λ configuration [25]. Thus we have two interfering cascade decay channels from the top state to the antisymmetric state $|4\rangle \rightsquigarrow |\pm\rangle |D\rangle$. The interference can be constructive or destructive depending on the coherence ρ_{+-}, which is induced by the coherent couplings on two cascade transitions $|D\rangle \leftrightarrow |\pm\rangle \leftrightarrow |4\rangle$ [Eqs. (20) and (21)]. Note that the coherent couplings are detuned from respective transitions by the detunings $\pm\frac{1}{2}\omega_{-+}$, which indicates that the coherence ρ_{+-} is determined by three effective parameters $\frac{\Omega_u}{\omega_{-+}}$, $\frac{\Omega_l}{\omega_{-+}}$, and $\frac{\gamma_1}{\omega_{-+}}$. When the interference is constructive, the middle state $|3\rangle$ (as the component of the dressed states $|\pm\rangle$) and/or the top state $|4\rangle$ become preferred radiative and almost unpopulated states. This increases the probability of returning the atom to these states from the lower states by the driving field and thus the probability of detecting a successive photon at time $\tau>0$ after detection of a photon at time $\tau=0$. Thus we have the strong correlations. When the interference is destructive, $|3\rangle$ and/or $|4\rangle$ are not preferred decaying states. In this case the atom tends to stay in the excited states $|3\rangle$ and/or $|4\rangle$ and not to decay, and this leads to the reduction of the probability of detecting a pair of photons at the successive times $\tau=0$ and $\tau>0$. As a result, we have the anticorrelations.

In summary, we have studied the photon correlations of the two fluorescent fields emitted from a driven cascade atom with lower-level splitting. In the different ranges of parameters, the strong correlations can be obtained for both fluorescent fields, anticorrelations for both, and strong correlation for one and anticorrelation for the other. The physical mechanism is attributed to the quantum interference between the two cascade transitions in the dressed states representation.

This work is supported by the National Natural Science Foundation of China under Grant No. 10574052.

[1] E. Arimondo, in *Progress in Optics*, edited by E. Wolf (Elsevier Science, Amsterdam, 1996), Vol. 35, pp. 257–354.
[2] S. E. Harris, Phys. Today **50** (7), 36 (1997).
[3] J. P. Marangos, J. Mod. Opt. **45**, 471 (1998).
[4] M. D. Lukin and A. Imamoglu, Nature (London) **413**, 273 (2001); M. D. Lukin, Rev. Mod. Phys. **75**, 457 (2003).
[5] M. Fleischhauer, A. Imamoglu, and I. P. Marangos, Rev. Mod. Phys. **77**, 633 (2003).
[6] O. Kocharovskaya, Phys. Rep. **219**, 175 (1992).
[7] M. O. Scully, Phys. Rep. **219**, 191 (1992).
[8] P. Mandel, Contemp. Phys. **34**, 235 (1994).
[9] J. Mompart and R. Corbalan, J. Opt. B: Quantum Semiclassical Opt. **2**, R7 (2000).
[10] S. Y. Zhu and M. O. Scully, Phys. Lett. A **201**, 85 (1995); S. Y. Zhu and M. O. Scully, Phys. Rev. Lett. **76**, 388 (1996); G. S. Agarwal, *ibid.* **84**, 5500 (2000).
[11] D. J. Gauthier, Y. Zhu, and T. W. Mossberg, Phys. Rev. Lett. **66**, 2460 (1991); H. R. Xia, C. Y. Ye, and S. Y. Zhu, *ibid.* **77**, 1032 (1996); L. Li, X. Wang, J. Yang, G. Lazarov, J. Qi, and A. M. Lyyra, *ibid.* **84**, 4016 (2000); J. Wang, H. M. Wiseman, and Z. Ficek, Phys. Rev. A **62**, 013818 (2000).
[12] P. Zhou and S. Swain, Phys. Rev. Lett. **77**, 3995 (1996); G. C. Hegerfeldt and M. B. Plenio, Phys. Rev. A **53**, 1164 (1996).
[13] E. Paspalakis and P. L. Knight, Phys. Rev. Lett. **81**, 293 (1998); C. H. Keitel, *ibid.* **83**, 1307 (1998); M. A. G. Martinez, P. R. Herczfeld, C. Samuels, L. M. Narducci, and C. H. Keitel, Phys. Rev. A **55**, 4483 (1997).
[14] P. R. Berman, Phys. Rev. A **58**, 4886 (1998); **72**, 035801 (2005); X. M. Hu, W. X. Shi, Q. Xu, H. J. Guo, J. Y. Li, and X. X. Li, Phys. Lett. A **352**, 543 (2006); Q. Xu, X. M. Hu, H. J Guo, J. Y. Li, X. X. Li, and W. X. Shi, Opt. Commun. **265**, 255 (2006).
[15] R. Loudon, *The Quantum Theory of Light* (Oxford University Press, Oxford, 1983).
[16] D. F. Walls and G. J. Milburn, *Quantum Optics* (Springer, Berlin, 1994).
[17] S. Swain, P. Zhou, and Z. Ficek, Phys. Rev. A **61**, 043410 (2000).
[18] Z. Ficek and S. Swain, Phys. Rev. A **69**, 023401 (2004).
[19] F. Wang and X. M. Hu, Chin. Phys. Lett. **24**, 432 (2007).
[20] X. M. Hu and F. Wang, Chin. Phys. Lett. **24**, 421 (2007).
[21] S. V. Lawande, R. R. Puri, and R. D'Souza, Phys. Rev. A **33**, 2504 (1986); H. Huang, S. Y. Zhu, M. S. Zubairy, and M. O. Scully, *ibid.* **53**, 1834 (1996).
[22] M. O. Scully and M. S. Zubairy, *Quantum Optics* (Cambridge University Press, Cambridge, England, 1997).
[23] M. Lax, Phys. Rev. **172**, 350 (1968).
[24] D. A. Cardimona, M. G. Raymer, and C. R. Stroud, Jr., J. Phys. B **15**, 55 (1982); M. Fleischhauer, C. H. Keitel, L. M. Narducci, M. O. Scully, S. Y. Zhu, and M. S. Zubairy, Opt. Commun. **94**, 599 (1992).
[25] J. Javanainen, Europhys. Lett. **17**, 407 (1992); X. M. Hu and J. S. Peng, J. Phys. B **33**, 921 (2000).